

Analytic approach to the critical density in cellular automata for traffic flow

M. Gerwinski and J. Krug*

Fachbereich Physik, Universität GH Essen, D-45117 Essen, Germany

(Received 12 February 1999)

The jamming transition in the stochastic traffic cellular automaton of Nagel and Schreckenberg [J. Phys. I **2**, 2221 (1992)] is examined. We argue that most features of the transition found in the deterministic limit do not persist in the presence of noise, and suggest instead to define the transition to take place at that critical density ρ_c at which a large initial jam just fails to dissolve. We show that $\rho_c = v_J / (v_J + v_F)$, where v_F is the velocity of noninteracting vehicles and v_J is the speed of the dissolution wave moving into the jam. An approximate analytic calculation of v_J in the framework of a simple renormalization scheme is presented, which explicitly displays the effect of the interaction between vehicles during the acceleration stage of the Nagel-Schreckenberg rules with maximum velocity $v_{\max} > 1$. The analytic prediction is compared to numerical simulations. We find a remarkable correspondence between the analytic expression for v_J and a phase diagram obtained numerically by Lübeck *et al.* [Phys. Rev. E **57**, 1171 (1998)]. [S1063-651X(99)05907-3]

PACS number(s): 05.40.-a, 89.40.+k, 05.60.-k

I. INTRODUCTION

The quantitative modeling of social processes is a conceptually challenging but also somewhat problematic task. Given the richness and unpredictability of human behavior, it seems that real progress can be expected foremost in situations where the actors' options are severely restricted. For example, a driver on a single lane road can react to her environment only by changing her speed, and she is further constrained by considerations of safety and traffic regulations. For this reason traffic simulations are a promising testing ground for attempts to extend statistical mechanics into an interdisciplinary science of complex, natural, and social systems. Previously the exclusive domain of engineers and traffic planners, the massive recent efforts in the statistical physics community have revealed fascinating analogies between vehicular traffic and other instances of nonequilibrium transport, most notably granular flow [1–3].

Much of this work has been devoted to understanding the qualitative difference between the regimes of high and low traffic density, and the possibility of a phase transition separating the two. Apart from the obvious practical interest in avoiding the spontaneous formation of traffic jams in the high density phase, the existence of a phase transition in one-dimensional, noisy nonequilibrium systems is a noteworthy feature in itself, since such transitions are impossible in thermal equilibrium [4].

In this paper we address the transition between the regimes of high and low density in the framework of a stochastic cellular automaton (STCA) for traffic flow originally proposed by Nagel and Schreckenberg [5]. In this model cars move on a single-lane road with periodic boundary conditions. Each car i has a discrete velocity $v_i \in \{0, \dots, v_{\max}\}$ and location x_i . The algorithm is described by the following rules.

- (1) All cars with $v_i < v_{\max}$ accelerate by 1: $v_i \rightarrow v_i + 1$.

- (2) Define the *headway* $g_i = x_{i+1} - x_i - 1$ as the number of empty cells in front of the car; then all cars with $v_i > g_i$ slow down to $v_i = g_i$.

- (3) With probability p , each car with $v_i > 0$ slows down by 1: $v_i \rightarrow v_i - 1$.

- (4) All cars move according to their current speed: $x_i \rightarrow x_i + v_i$.

Here, v_{\max} is the maximum velocity cars are able (or allowed) to drive, whereas the randomization step involving p describes the tendency of drivers to delay acceleration or to overreact in braking; p will be referred to as the *delay probability*. Typical values to model highway traffic are $v_{\max} = 5$, $p = 0.3$. In addition to the model parameters v_{\max} and p , the behavior depends on the car density $\rho = N/L \in [0, 1]$, where N is the number of cars on the ring and L the number of lattice sites. Despite its simplicity, this algorithm already shows a lot of features observed in real traffic [1,2,5,6].

In the deterministic limit ($p = 0$) the Nagel-Schreckenberg model displays a sharp transition between free and congested flow at a density $\rho_c^0 = 1/(v_{\max} + 1)$ [7]. The main features of this transition are summarized in the next section, along with some new conjectures and results pertaining to the relaxation behavior into the (periodic) steady state. Section III critically examines the (currently open) question of how much of the transition in the deterministic cellular automaton survives in the presence of noise, and some obvious ways of characterizing the transition in the noisy STCA are ruled out. In Sec. IV A we suggest a definition of the critical density ρ_c in terms of the dissolution of a large traffic jam (a ‘‘megajam’’), which applies to the noisy as well as to the deterministic model. We derive an expression for ρ_c containing two characteristic velocities: The free-flow velocity v_F , and the jam dissolution speed v_J . Section IV B is devoted to an approximate calculation of v_J using a simple renormalization argument to treat the interactions between vehicles leaving a jam. Subsequently, the analytic results for ρ_c are compared with numerical data in Sec. IV C, and the paper is concluded with a discussion of our results in comparison to other recent approaches.

*Author to whom correspondence should be addressed. Electronic address: jkrug@theo-phys.uni-essen.de

II. DETERMINISTIC CELLULAR AUTOMATON

A. Steady state

When the random braking probability p is set to zero, the STCA becomes a deterministic cellular automaton (CA). Starting from an arbitrary initial condition on a finite lattice, a time-periodic steady state is reached in finite time [7]. The dynamical rules for $p=0$ can be written as

$$\begin{aligned} v_i(t) &= \min[v_{\max}, v_i(t-1) + 1, g_i(t)], \\ x_i(t+1) &= x_i(t) + v_i(t). \end{aligned} \quad (1)$$

Two types of steady state solutions exist, depending on the value of the density ρ . For densities below the critical density

$$\rho_c^0 = \frac{1}{v_{\max} + 1} \quad (2)$$

one may choose the g_i such that $g_i \geq v_{\max}$ for all i , and hence Eq. (1) is satisfied by

$$v_i(t) \equiv v_{\max}, \quad \rho < \rho_c^0. \quad (3)$$

For $\rho > \rho_c^0$ the relevant solutions are characterized by

$$v_i(t) = g_i(t), \quad \rho > \rho_c^0. \quad (4)$$

This solves Eq. (1) provided $g_i \leq v_{\max}$ for all i , and also $v_i(t) \leq v_i(t-1) + 1$. The latter condition is simplified by noting that Eq. (4) implies $v_i(t) = v_{i+1}(t-1)$, i.e., the entire velocity configuration is shifted to the left in each time step [7]. Thus a steady state solution of the type (4) is realized if and only if the configuration of headways satisfies $g_i \leq \min[v_{\max}, g_{i-1} + 1]$. Note that at the critical density ρ_c^0 the only steady state solution (up to translations) is the ordered configuration with all headways equal to v_{\max} .

The critical density ρ_c^0 is thus used to separate two qualitatively different flow regimes: For $\rho < \rho_c^0$ the cars move freely at the velocity $v_F = v_{\max}$, while for $\rho > \rho_c^0$ their speed is completely determined by the headways [Eq. (4)]. A natural order parameter distinguishing the two regimes is the fraction of jammed vehicles (defined, e.g., as vehicles with velocities less than v_{\max} [8]). Unfortunately in the deterministic model this and related quantities depend on the initial spatial distribution of cars. In contrast, the average velocity $v(\rho)$ and, correspondingly, the steady state current (or *fundamental diagram* [1–3]) $j(\rho) = \rho v(\rho)$ can be read off from eqs. (3) and (4) by noting that the average headway equals $1/\rho - 1$. The result [7]

$$j(\rho) = \min[v_{\max}\rho, 1 - \rho] \quad (5)$$

is a piecewise linear function with a singularity (a discontinuity in the first derivative) at the critical density ρ_c^0 , which coincides with the density of maximum flow. An order parameter $\phi(\rho)$ can then be defined as the deviation of the average velocity from the velocity $v_F = v_{\max}$ of freely moving cars,

$$\phi(\rho) \equiv v_F - v(\rho) = \min[0, (\rho - \rho_c^0)/\rho_c^0]. \quad (6)$$

B. Relaxation dynamics

While the steady state behavior of the deterministic CA is simple, the relaxation from general (random) initial conditions shows a certain complexity. The case $v_{\max} = 1$, where the model reduces to the elementary CA No. 84 in Wolfram's classification [9], has been analyzed in great detail [10–12]. The key step is a transformation in which adjacent pairs of vacant lattice sites map to particles moving ballistically at velocity $+1$, and pairs of sites occupied by cars map to antiparticles moving at velocity -1 . Particles and antiparticles annihilate upon collision. The initial condition determines the initial densities ρ_+ and ρ_- of particles and antiparticles. The ‘‘charge density’’ $\rho_+ - \rho_-$ is conserved under collisions, and is related to the density ρ of the CA through $\rho_+ - \rho_- \sim \rho_c^0 - \rho$. At the critical point $\rho_+ = \rho_-$ the pairwise annihilation proceeds to completion, while for $\rho < \rho_c^0$ ($\rho > \rho_c^0$) an excess of particles (antiparticles) remains.

Translating known results for the ballistic annihilation process [10,13] leads to a number of predictions for the relaxation behavior of the CA in the case of random initial conditions with short-ranged correlations. In the infinite system the approach of the order parameter (6) to its steady state value is exponential with a characteristic time scale $\tau(\rho)$ which diverges as

$$\tau \sim |\rho - \rho_c^0|^{-2}, \quad \rho \rightarrow \rho_c^0 \quad (7)$$

while at the critical point

$$\phi(t) \sim t^{-1/2}, \quad \rho = \rho_c^0. \quad (8)$$

Finite size effects are governed by the ratio of the system size L to a dynamic correlation length which grows linearly in t . Consequently the relaxation time is affected by the system size when $\tau(\rho) \sim L$ or $|\rho - \rho_c^0| \sim L^{-1/2}$; at the critical point $\tau \sim L$. These relations can be summarized in a finite size scaling form, which is expected to hold for $L \gg 1$ and $|\rho - \rho_c^0| \ll 1$,

$$\tau(\rho, L) = LF(L(\rho - \rho_c^0)^2), \quad (9)$$

with $F(0) = \text{const}$ and $F(s \rightarrow \infty) \sim 1/s$.

It is not known if an exact mapping to ballistic annihilation exists for other values of v_{\max} . However, inspection of the time evolution of the CA suggests a similar scenario as in the case $v_{\max} = 1$: When viewed as ‘‘defects’’ in the ordered steady state configuration $g_i \equiv v_{\max}$, which the system approaches at $\rho = \rho_c^0$, clusters of vacancies move forward at speed v_{\max} and clusters of excess cars move backwards at speed 1. Due to the existence of several velocity states the clusters of excess cars have a more complicated internal structure, and the collisions with vacancy clusters are difficult to entangle. Nevertheless the basic features of a ballistic annihilation process with two velocities [14] are still present, and it seems likely that the relaxation process can still be described in terms of the scaling laws (7)–(9). Indeed, the numerical data for the relaxation time $\tau(\rho, L)$ presented by Nagel and Herrmann [7] for $v_{\max} = 5$ appear to be consistent with the scaling form (9), in particular, the relation $\tau(\rho_c^0, L) \sim L$ was verified. In Fig. 1 we show simulation results for the relaxation of the number of jammed cars at the

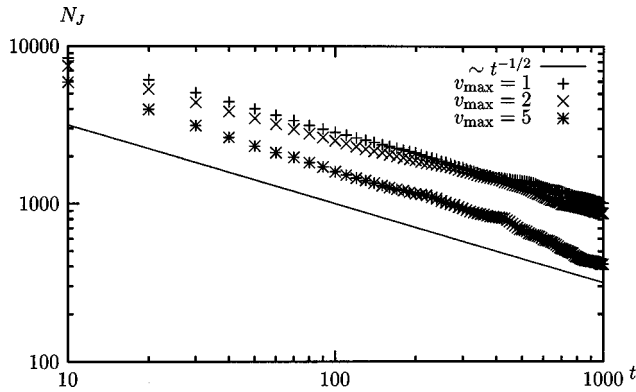


FIG. 1. Simulation data for the number N_j of jammed vehicles (vehicles with velocity $v < v_{\max}$) for the deterministic CA with $v_{\max} = 1, 2$, and 5 . The initial condition was a random distribution of cars with density ρ_c^0 . The data were obtained in single runs of systems of size $L = 10^5$. The full line indicates the predicted $t^{-1/2}$ decay.

critical point for $v_{\max} = 1, 2$, and 5 , which support the universality of the power law (8).

III. CRITERIA FOR A PHASE TRANSITION IN THE PRESENCE OF NOISE

We have seen above that the deterministic CA displays a phase transition at a well-defined critical density ρ_c^0 , which can be identified through the following three features. (1) The fundamental diagram $j(\rho)$ has a singularity at ρ_c^0 , which also coincides with the density of maximum flow. (2) An order parameter $\phi(\rho)$ related to the density of jammed cars exists, which vanishes for $\rho < \rho_c^0$. (3) The relaxation time into the steady state diverges (or rather, becomes system-size dependent) at $\rho = \rho_c^0$.

The key question, which has been intensely debated in the recent literature [15–22], is whether any of these features persist in the presence of stochasticity ($p > 0$), and if so, whether they can be taken as an indication for the existence of a sharp phase transition. In the following we will argue that the answer to both questions is probably negative, and that therefore another definition of the critical density is called for. This will then be provided in Sec. IV A. We will discuss the three features (1)–(3) separately. Some other recent attempts to characterize the transition, which are closely related to our own approach, will be mentioned in Sec. III D.

A. Fundamental diagram

The exact solution for the case $v_{\max} = 1$ [23,24] shows that the fundamental diagram $j(\rho)$ becomes analytic for any nonzero random braking probability $p > 0$. Mean field calculations [25] and numerical measurements indicate that this is true also for $v_{\max} > 1$. Two cautionary remarks are, however, in order. First, a weak singularity in $j(\rho)$ may be difficult to detect numerically, as is illustrated by the case of exclusion models with random jump rates, for which the existence of a phase transition is rigorously established [26]. Second, numerical measurements of $j(\rho)$ at large values of v_{\max} tend to show spurious features near the density of maximum flow, which seem to be caused by surprisingly strong finite size effects (Fig. 2).

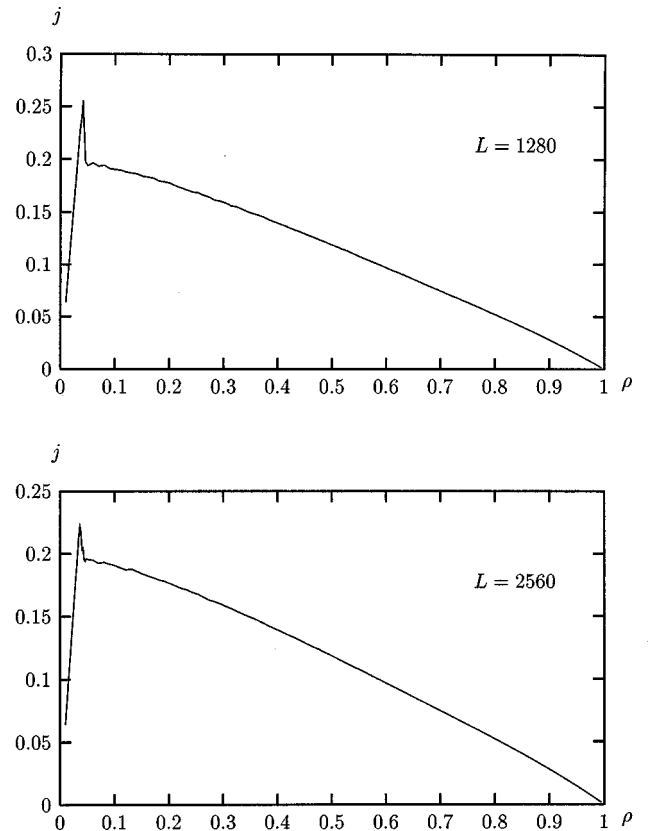


FIG. 2. Numerically determined fundamental diagrams of the STCA with $v_{\max} = 7$ and $p = 0.7$. Comparison of the data for $L = 1280$ (upper panel) and $L = 2560$ (lower panel) shows that the sharp feature near maximum flow is a finite size effect.

Even if the fundamental diagram is smooth, it always possesses a maximum at some density ρ_{\max} , which is an obvious candidate for a critical density separating different flow regimes. In the deterministic case we have seen that $\rho_{\max} = \rho_c^0$, and in general ρ_{\max} is distinguished as the density where the drift velocity $c = j'(\rho)$ of perturbations changes its sign [27]. We will return to the question of the relationship between ρ_{\max} and ρ_c below in Sec. IV A.

B. Order parameter

According to the STCA rules, a freely moving car switches randomly between the velocities v_{\max} and $v_{\max} - 1$. States with lower velocities can be reached only through the mutual interactions between cars: To slow down to $v_{\max} - 2$ an encounter with one randomly braking car ahead is required, to reach $v_{\max} - 3$ two cars have to be within interaction range, and so on. Due to the random fluctuations in the motion of individual cars close encounters of an arbitrary number of vehicles occur with finite probability. More precisely, the probability for n cars to be found in close vicinity of a given car is proportional to ρ^n , and consequently the probability $P_v(\rho)$ of finding a car with velocity $v < v_{\max} - 1$ should behave as

$$P_v(\rho) \sim \rho^{v_{\max} - 1 - v} \quad (10)$$

for $\rho \rightarrow 0$. This rough argument illustrates that any order parameter related to the fraction of jammed vehicles—e.g., the

fraction of standing cars [15,16] or the fraction of cars with velocity below $v_{\max}-1$ —is nonzero at any density $\rho > 0$, and hence cannot be used to identify a possible phase transition [16]. Since the average velocity $v(\rho)$ is determined by the velocity distribution $P_v(\rho)$, the same is true for the order parameter $\phi(\rho)$ defined in Eq. (6).

C. Relaxation time

Csányi and Kertész pointed out that a suitably defined relaxation time shows a sharp peak near but below the density of maximum flow [17]. Subsequent work has confirmed this behavior, but the nature of the divergence and its dependence on system size seems difficult to determine [16,18]. In fact, using the divergence of the relaxation time to identify a phase transition is problematic for a fundamental reason: In a stochastic model with a conservation law, the relaxation time (properly defined, e.g., through the gap in the spectrum of the time evolution operator) depends on the system size as $\tau \sim L^z$ for any nonzero density. Here z is the dynamic exponent, which for driven diffusive systems in one dimension, such as the STCA, takes the value $z=3/2$. This result has been derived in the framework of a nonlinear fluctuating continuum equation for the particle density [28], which is equivalent to the one-dimensional noisy Burgers equation [29] also known as the Kardar-Parisi-Zhang (KPZ) equation of surface growth [30]; some numerical evidence for KPZ scaling in the STCA has been presented by Sasvári and Kertész [18]. The value $z=1$ of the dynamic exponent of the *deterministic* model at $\rho=\rho_c^0$ [Eq. (9)] is related to the cusp of the fundamental diagram; for a smooth fundamental diagram and random initial conditions one expects $z=3/2$ instead, see [10] for a detailed discussion.

Thus, the density dependent features of τ observed numerically [16–18] are due partly to a nonstandard definition of the relaxation time, and partly reflect the density dependence of the prefactor in the relation $\tau \sim L^z$. They should not, however, be interpreted as a critical slowing down analogous to the scaling laws (7) and (9) in the deterministic case.

D. Spatial structure

Several recent papers have attempted to distinguish between the high and low density flow regimes by directly characterizing the spatial structure as a function of the global density. Eisenblätter *et al.* [16] measured the density-density correlation function. The correlation length $\xi(p, \rho)$ was found to be finite for all $p > 0$, with a maximum value ξ_{\max} attained near ρ_{\max} which diverges in the deterministic limit as

$$\xi_{\max} \sim p^{-1/2}. \quad (11)$$

This behavior, which can be derived analytically for $v_{\max}=1$ [16], has a simple interpretation in terms of the ballistic annihilation picture proposed in Sec. II B. For small values of p and densities near ρ_c^0 the random braking events create pairs of defects [31]—a small jam and a cluster of vacancies—in the ordered structure of equally spaced cars which constitutes the steady state at $p=0$, $\rho=\rho_c^0$. The analysis of two-species ballistic annihilation with pair creation [32] shows that the stationary defect density scales as

the square root of the defect creation rate. Identifying the correlation length ξ_{\max} with the average spacing between defects, Eq. (11) follows. The fact that Eq. (11) holds independent of the value of v_{\max} [16] lends further support to the applicability of ballistic annihilation for general v_{\max} .

The visual appearance of space-time plots showing the trajectories of cars for $v_{\max} > 1$ and $\rho > \rho_{\max}$ indicates the spatial coexistence of freely flowing and jammed regions [6,25]. Some quantitative support for this view has been provided in recent work by Chowdhury *et al.* [19] and Lübeck *et al.* and Roters [20,21], who found double-peaked probability distributions of headways [19] and local densities [20,21] for a range of global densities. Lübeck *et al.* and Roters [20,21] used the first appearance of the double-peak structure to identify a critical density, which will be compared to our definition of ρ_c below in Sec. V.

The analogy to thermodynamic phase coexistence suggests defining ρ_c as the density at which droplets of the congested phase—that is, traffic jams—are marginally stable. This picture forms the basis of the analytic approach to be described in the next section.

IV. DISSOLUTION OF A MEGAJAM

A. The critical density

Our goal in this section is to provide a simple and unambiguous distinction between the free-flow low density regime and the interaction-dominated regime at high densities. An intuitively plausible criterion for interaction-dominated flow is the existence of traffic jams which never dissolve. We postpone a detailed discussion of jam dissolution times to Sec. IV C, and consider here a simplified situation where the system is started in a “megajam” initial condition [8,33]: At time $t=0$, a block of N sites is filled with cars at velocity $v_i=0$, while the remaining $L-N$ sites are empty. Assuming uniqueness of the stationary state of the STCA, the survival of such a megajam should be equivalent to the occurrence of jams with infinite lifetimes for arbitrary initial conditions.

Space-time plots of the time evolution for different values of $\rho=N/L$ are shown in Fig. 3. Obviously a sufficient condition for the megajam to dissolve is that the last car in the jam has started to move before the first car reaches the back end of the jam. The dissolution can be described in terms of a dissolution wave which moves into the jam at velocity v_J . The position of the dissolution wave marks the transition between standing and moving cars; for a precise definition see Sec. IV B. The first car moves freely, and therefore (after a finite acceleration period) its speed is v_{\max} ($v_{\max}-1$) with probability $1-p$ (p), leading to the average *free-flow velocity*

$$v_F = v_{\max} - p. \quad (12)$$

We conclude that the condition for the first car to reach the back end of the jam at the same time as the dissolution wave reads $(L-N)/v_F = N/v_J$. This will be taken as the definition of the critical density ρ_c , which is therefore given by

$$\rho_c = \frac{v_J}{v_J + v_F} = \frac{v_J}{v_J + v_{\max} - p}. \quad (13)$$

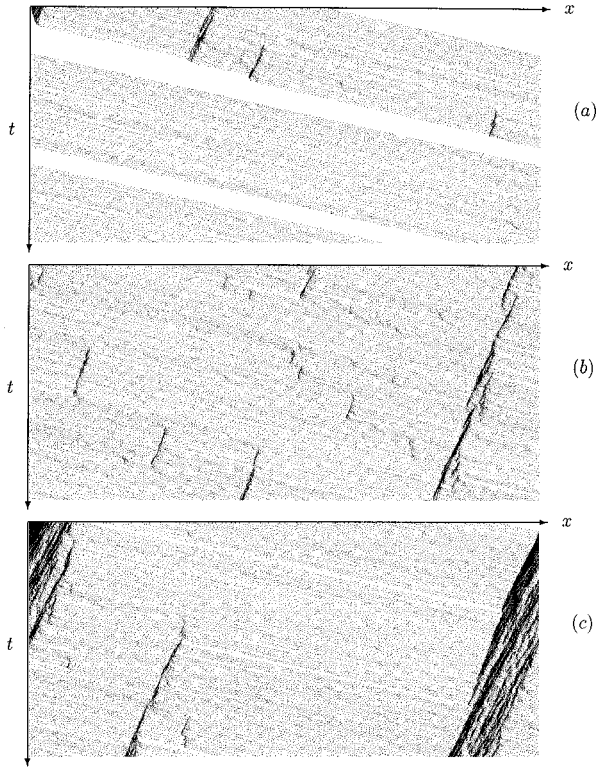


FIG. 3. Space-time diagrams for the STCA with $v_{\max}=5$, $p=0.3$, starting from a megajam initial condition. The mean density $\rho=N/L$ in the three panels is (a) $\rho=0.8\rho_c$, (b) $\rho=\rho_c$, and (c) $\rho=1.2\rho_c$, where $\rho_c\approx 0.1097$ is the theoretically predicted critical density (21). The depicted time evolution starts at the time N/v_J at which the jam dissolution wave reaches the end of the initial jam. In the upper left corner of (a) the last piece of the dissolving jam can be seen. Subsequently the system evolves into a block of cars at a density near ρ_c which move freely, and a gap of vacancies which will eventually close due to fluctuations. In (b) a thin trace of the jam is seen to survive in the right part of the figure throughout the depicted time evolution, while in (c) the initial jam clearly does not dissolve.

The nontrivial quantity in this equation is the jam dissolution velocity v_J . If the acceleration to v_{\max} occurred instantaneously, as is the case for $v_{\max}=1$, we would simply have $v_J=1-p$ (see Sec. IV B), and Eq. (13) would reduce to

$$\rho_c^> = \frac{1-p}{v_{\max}+1-2p}. \quad (14)$$

However, due to delays in the acceleration phase, v_J is generally smaller than $1-p$, and consequently Eq. (14) provides only an *upper* bound on the true critical density. This will be explicitly displayed by the approximate calculation in the next section. Here we remark that the expression (14) has a number of features in common with the true critical density. (i) It reduces to Eq. (2) in the deterministic limit $p\rightarrow 0$. (ii) For $v_{\max}=1$ it yields $\rho_c=1/2$ independent of p , which should be true because of particle-hole symmetry in that case. (iii) At fixed $v_{\max}\geq 2$ it shows the numerically observed *decrease* of ρ_c with increasing p .

Equation (14) also has a natural interpretation in terms of the fundamental diagram $j(\rho)$. Note that $j(\rho)$ is known exactly in the limits $\rho\rightarrow 0$ and $\rho\rightarrow 1$ [15]: For low densities

TABLE I. Numerical results for the density of maximum flow, ρ_{\max} , in comparison with the approximate analytic expressions (14) and (21) for the critical density for jam dissolution, and the expression (16) for the density of maximum flow.

v_{\max}	p	$\rho_c^>$	ρ_c	ρ_{\max}	$\rho_{\max}^{(E)}$
2	0.3	0.292	0.254	0.303	0.233
2	0.5	0.250	0.216	0.259	0.167
2	0.7	0.188	0.168	0.202	0.100
3	0.3	0.206	0.177	0.204	0.175
3	0.5	0.167	0.142	0.159	0.125
3	0.7	0.115	0.103	0.110	0.075
4	0.3	0.159	0.135	0.145	0.140
4	0.5	0.125	0.106	0.110	0.100
4	0.7	0.0833	0.0737	0.0691	0.0600
5	0.3	0.130	0.110	0.113	0.117
5	0.5	0.100	0.0843	0.0770	0.0833
5	0.7	0.0652	0.0576	0.0500	0.0500

cars do not interact, hence $j\approx v_F\rho$ for $\rho\rightarrow 0$, while for very high densities only single vacancies move backwards at speed $1-p$, and therefore $j\approx(1-p)(1-\rho)$ for $\rho\rightarrow 1$. Extrapolating these two relations up to their crossing point we obtain a piecewise linear fundamental diagram, which generalizes Eq. (5) to $p>0$; provided $j(\rho)$ is convex, this function is an upper bound to the true fundamental diagram,

$$j(\rho)\leq\min[(v_{\max}-p)\rho,(1-p)(1-\rho)]. \quad (15)$$

The maximum of the right hand side occurs precisely at $\rho_c^>$, which should therefore be close to the density of maximum flow ρ_{\max} at least for small p . This is confirmed by the data in Table I, where numerically determined values of ρ_{\max} are compared to the expressions (14) and (21). It is interesting to note that ρ_{\max} tends to decrease relative to $\rho_c^>$ and ρ_c with increasing p . Table I also contains the expression

$$\rho_{\max}^{(E)} = \frac{1-p}{v_{\max}+1} \quad (16)$$

due to Eisenblätter [34], which was quoted by Lübeck *et al.* [20]. Equation (16) describes the numerical data for ρ_{\max} quite well for large v_{\max} ($v_{\max}=4,5$) but our expressions (14) and (21) are superior for smaller values of v_{\max} .

B. Renormalization of the dissolution speed

To compute the jam dissolution speed v_J we first require a reasonable definition of the jam dissolution wave and, consequently, a reasonable definition of a jam. Here we will call a car ‘‘jammed’’ if it is moving at any velocity $v<v_{\max}$ [8]. This is motivated by the observation that a car with $v=v_{\max}$ cannot interact with cars behind it, while a slower car can make them decelerate in order to avoid a crash. Thus our definition amounts to calling a car jammed, if it is able to jam other cars itself. Correspondingly, we say that a car *leaves* the megajam when it first reaches velocity v_{\max} , starting from velocity 0. The location of the jam dissolution wave is therefore defined as the location of the car which is currently leaving the jam.

We first adopt the following simplified view of jam dissolution: At time $t=0$ all cars are standing in a megajam of unit density. Each car starts with a time delay τ_D after the car ahead is gone, and then accelerates constantly. Then the velocity of the jam dissolution wave is simply τ_D^{-1} . For the STCA with $v_{\max}=1$, this scenario is exactly realized: Each car at rest with an empty cell in front of it has a probability of $q=1-p$ to start in the next time step, thus the average waiting time is $\tau_D=q^{-1}$ and

$$v_J = q = 1 - p. \quad (17)$$

In the following q will be referred to as the *acceleration rate*.

For $v_{\max} > 1$ the situation is more complicated: Because of the finite acceleration times, interaction may arise between the cars before reaching v_{\max} , so the assumption of constant acceleration is invalidated. We can nevertheless calculate the average acceleration time T it takes a car to reach maximum velocity, and define an *effective acceleration rate* through

$$q_{\text{eff}} = \frac{v_{\max}}{T}. \quad (18)$$

For the first car leaving the jam $q_{\text{eff}} = q$, while for subsequent cars q_{eff} decreases because their acceleration is impeded by the car ahead; correspondingly the jam dissolution wave slows down as it moves into the megajam. The macroscopic jam dissolution velocity v_J entering Eq. (13) is determined by the limiting value q^* of q_{eff} deep inside the jam.

Our approximate computation of q^* proceeds iteratively. Let us label the cars by $i=1,2,3,\dots$, from the front of the megajam backward. We assume that the effective acceleration rate $q_{\text{eff}}(i)$ of car i can be obtained from its intrinsic acceleration rate $q=1-p$ and the effective acceleration rate $q_{\text{eff}}(i-1)$ of the car ahead by treating the latter as a *free* car with delay probability $p'=1-q_{\text{eff}}(i-1)$. In essence, we assume that the effects of the cars further ahead in the jam can be lumped into a single, *renormalized* delay probability. This reduces the calculation to a two-particle problem, which can be solved analytically (see Appendix A). For $v_{\max}=2$ one obtains the recursion

$$q_{\text{eff}}(i) = 2q \left(1 - \frac{1}{2 - q + q q_{\text{eff}}(i-1)} \right). \quad (19)$$

It is easy to check that the map (19) has a unique, attractive fixed point $q^* \leq q$, which defines the acceleration rate deep inside the jam and is given by

$$q^* = \frac{1}{2q} \left[\sqrt{(2-q-2q^2)^2 + 8q^2(1-q)} - (2-q-2q^2) \right]. \quad (20)$$

The function $q^*(p)$ is displayed in Fig. 4. It joins the line $q=1-p$ tangentially at $p=1$ but at a finite angle at $p=0$. Expanding Eq. (20) yields $q^* \approx (1-p) - (1-p)^2/2$ for $p \rightarrow 1$ and $q^* \approx 1-2p$ for $p \rightarrow 0$. Our final prediction for ρ_c is obtained by setting $v_J = q^*$ in Eq. (13),

$$\rho_c(v_{\max}, p) = \frac{q^*(p)}{q^*(p) + v_{\max} - p}. \quad (21)$$

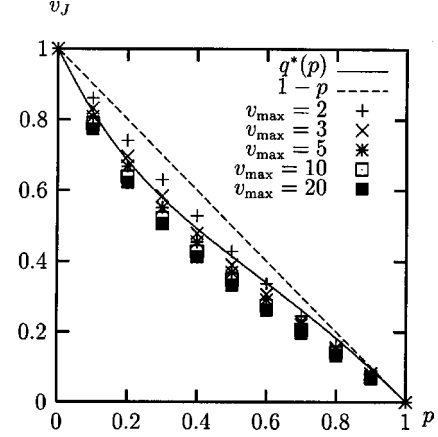


FIG. 4. Numerical data for the jam dissolution speed v_J compared to the analytic prediction (20) (shown as a solid line). The measurement algorithm is described in Appendix B. Each data point is an average over 100 runs.

Equations (20) and (21) constitute the central results of this paper.

Higher values of v_{\max} can in principle be treated in a similar way, but we have not pursued this because the complexity of the two-particle problem grows as $4^{v_{\max}}$. As we will see below, the jam dissolution speed v_J depends only weakly on v_{\max} (provided $v_{\max} > 1$), and therefore Eqs. (20) and (21) provide a useful approximation also for $v_{\max} > 2$. In the next section Eqs. (20) and (21) will be compared to numerical data.

C. Numerical simulations of jam dissolution

We have numerically determined the jam dissolution speed v_J through simulations of megajams of length $N=5000$ in an infinite system (see Appendix B). The results are presented in Fig. 4, along with the analytic expression (20). As expected, $v_J = 1 - p$ for $v_{\max} = 1$ (data not shown) and $v_J < 1 - p$ for $v_{\max} \geq 2$. The quantitative agreement with the analytic expression (20) is best for $v_{\max} = 3$, while for $v_{\max} = 2$ (the case actually considered in our calculation) it seems to overestimate the reduction of v_J due to vehicular interactions. Simulations for large v_{\max} indicate the existence of a limiting curve $v_J(p)$ for $v_{\max} \rightarrow \infty$, implying that the acceleration time T scales as v_{\max} for large v_{\max} .

In Fig. 5 we show numerical results for the jam dissolution time τ_J (defined precisely in Appendix B) for the case of periodic boundary conditions. The observed behavior is rather more complicated than the simple picture adopted in Sec. IV A: While τ_J displays a sharp increase near the critical density ρ_c predicted by Eq. (21), it becomes “infinite” (in the sense that the jam does not dissolve within the measurement time) only beyond a second limiting density ρ'_c which is considerably larger than the maximum flow density ρ_{\max} [35]. In the intermediate density range $\rho_c < \rho < \rho'_c$ the jam does not dissolve during the first lap (after a time of the order of L), but it dissolves later due to fluctuations of the two ends of the jam. This is consistent with the observation of Nagel [8] of a size independent, large cutoff in the lifetime distribution for traffic jams at densities far beyond ρ_{\max} . For densities between ρ'_c and ρ_c other jams have usually formed

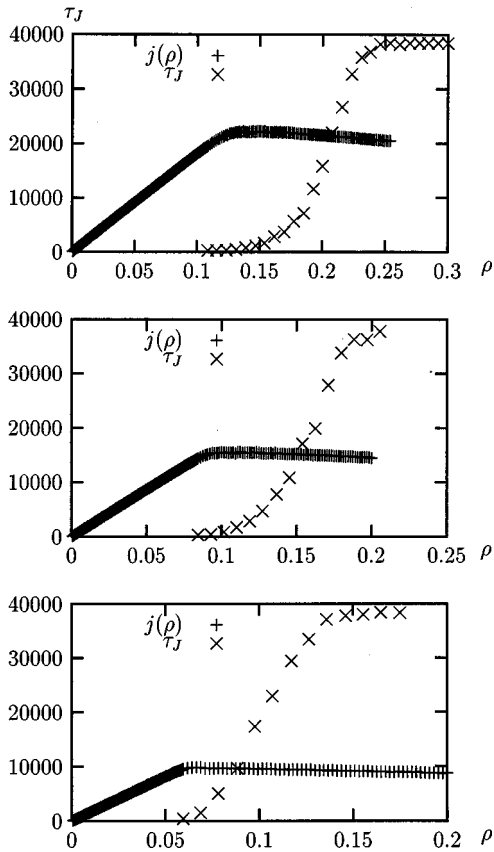


FIG. 5. The numerically determined megajam dissolution time $\tau_J(\rho)$ for $v_{\max}=4$ and $p=0.3$ (top panel), $p=0.5$ (middle), and $p=0.7$ (bottom). The system size was $L=1280$. The numerical procedure is described in Appendix B. Data for the fundamental diagram $j(\rho)$ are included to illustrate the vicinity of ρ_c and ρ_{\max} . For densities below ρ_c the dissolution time is essentially zero on the scale of the figure.

by the time the megajam dissolves. Therefore our expression (21) nevertheless provides a good estimate for the onset of congested traffic.

V. DISCUSSION AND SUMMARY

The occurrence of two characteristic velocities in the congested phase of the STCA was observed recently by Roters and co-workers in an analysis of the dynamic structure factor $S(k, \omega)$ of the model [21,22]. Two propagating modes appear as ridges in the (k, ω) plane. The speed of the forward propagating mode was identified as the free-flow velocity (12), while the speed v_j of the backward propagating wave seems to be closely related to the jam dissolution speed v_j considered in the present work. In particular, the numerically determined dependence of v_j on the delay parameter p is remarkably similar to that of the function $q^*(p)$ derived in Sec. IV B: v_j is less than $1-p$ and joins the line $1-p$ tangentially at $p=1$ but at a finite angle at $p=0$. The quantitative agreement is less impressive, since Roters *et al.* find v_j to be essentially independent of v_{\max} , while our data indicate a clear decrease of v_j with increasing v_{\max} (which, however, saturates for large v_{\max}). Nevertheless it is clear that closely related processes must take place both in the dissolution of a

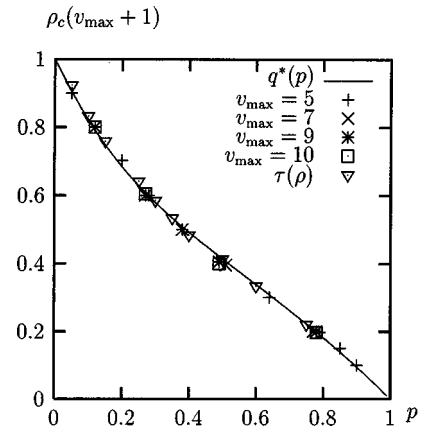


FIG. 6. The figure superimposes numerical data for the critical density ρ_c obtained from the density dependence of the relaxation time [34] (triangles) and from an analysis of local density fluctuations [21] (all other symbols) with the analytic expression (20), to illustrate the remarkable similarity between $q^*(p)$ and the function $f(p) = \rho_c(v_{\max} + 1)$ [Eq. (22)].

megajam, and in the inhomogeneous steady state flow in the congested phase.

Lübeck *et al.* and Roters [20,21] have presented a phase diagram for the STCA based on an analysis of the distribution of density fluctuations (see Sec. III D). The critical density at which this distribution first displays a bimodal structure characteristic of two-phase coexistence was found to be of the form

$$\rho_c = \frac{f(p)}{v_{\max} + 1}, \quad (22)$$

where f depends on the delay parameter p but *not* on v_{\max} . Our expression (13) can be brought into the form (22) only at the expense of adopting a rather awkward dependence of v_j on v_{\max} and p , and it is clearly inconsistent with this form if v_j is assumed to be independent of v_{\max} . Nevertheless Eq. (13) approaches the form (22) for large v_{\max} , with $f(p) = v_j$. Motivated by this observation, we compare in Fig. 6 the numerically determined function $f(p)$ [20,21,34] to our expression (20) for $v_j(p)$. The excellent agreement is probably fortuitous, but nevertheless intriguing. Perhaps an analysis of the limit $v_{\max} \rightarrow \infty$ would clarify its significance.

In conclusion, we have shown how quantitative estimates for the critical density ρ_c separating free and congested flow can be obtained from simple considerations of jam dissolution. While the nature of the transition occurring at ρ_c has not been addressed in this work, we feel that our analysis does shed some light on the role that the microscopic processes of acceleration and stochastic delay play in determining the critical density, and, thus, the maximum flow capacity of the model.

ACKNOWLEDGMENT

We thank L. Roters for providing us with the data for Fig. 6, and for making his thesis [21] available to us.

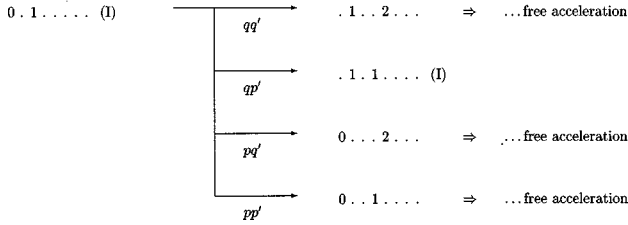


FIG. 7. Probability tree for the calculation of q_{eff} for the STCA with $v_{\text{max}}=2$. The figure illustrates the possible time evolution histories starting from the initial condition (I). Each car is denoted by a number giving its current velocity, and empty sites are denoted by dots.

APPENDIX A: SOLUTION OF THE TWO-VEHICLE PROBLEM

To derive the recursion relation (19) we consider a (free) *leading* car with delay probability p' (acceleration rate $q' = 1 - p'$) followed by a *trailing* car with delay probability p (acceleration rate $q = 1 - p$). Our goal is to compute the average number of time steps $T(p, p')$ required for the trailing car to first reach the maximum velocity $v_{\text{max}}=2$, given that at $t=0$ it was able to move for the first time. This implies that at $t=0$ the leading car has moved one step, and thus its velocity is $v' = 1$ and it is separated from the (standing) trailing car by a gap of size $g = 1$ (Fig. 7).

The subsequent time evolution of the two-vehicle system is a Markov chain in the space of variables (v, v', g) with the transition probabilities given in Fig. 7. We note that the gap g cannot decrease during the acceleration period (i.e., before $v = v_{\text{max}}$ for the first time). This is because a decrease in the gap requires $v > v'$, and since the leading car is free, its velocity satisfies $v' \geq v_{\text{max}} - 1 = 1$ for all times. On the other hand, an interaction between the two cars occurs only if $g < v_{\text{max}}$. Since three of the four transitions depicted in Fig. 7 lead to $g \geq v_{\text{max}} = 2$ in the first time step, in these cases the subsequent acceleration of the trailing vehicle is free, and the time required is simply $[v_{\text{max}} - v(1)]/q$, where $v(1)$ is the velocity of the trailing vehicle after the first step.

The only case where the vehicles continue to interact is when the trailing car accelerates but the leading car does not (the second transition in Fig. 7). In that case the resulting configuration after one time step is in fact *equivalent* to the initial configuration (I), since the velocity of the trailing vehicle will be set to $g = 1$ after the acceleration step, and hence it will be the same as if the car had started at $v = 0$ and accelerated. More generally, two configurations of the two-vehicle system can be seen to be equivalent in this sense if

(1) the gap size g and the velocity $v'(t)$ of the leading car are the same in both configurations, and (2) the trailing car has velocity $v(t) \geq g - 1$ in both configurations. Since the acceleration time out of two equivalent configurations is the same, the acceleration time out of the configuration .1.1... is equal to the acceleration time T from the initial configuration.

Summing over the four possible transitions in Fig. 7 we thus arrive at the equation

$$\begin{aligned} T &= 1 + qq'(1/q) + qp'T + pq'(2/q) + pp'(2/q) \\ &= 1 + q' + qp'T + 2p/q \end{aligned} \quad (\text{A1})$$

for the acceleration time T , which gives

$$\frac{1}{T} = \frac{1 - qp'}{1 + q' + 2p/q} = q \left(1 - \frac{1}{2 - q - qq'} \right). \quad (\text{A2})$$

Inserting this into Eq. (18) yields the recursion (19).

APPENDIX B: NUMERICAL ALGORITHMS

(a) *Measurement of v_J* . To measure v_J , a megajam of length $N = 5000$ was watched during dissolution on an infinite road. The measuring time t was set to zero, when the first car had reached $v = v_{\text{max}}$. The dissolution time T_J was the time when the last car reached $v = v_{\text{max}}$. v_J was then calculated as $v_J = N/T_J$.

(b) *Measurement of τ_J* . To measure the megajam dissolution time τ_J , the system has to be initialized with megajam initial conditions, i.e., all cars standing in one big cluster of density 1. Starting from these conditions, we now keep watching the index f of the foremost car and the length l of the megajam. Each time step the following algorithm is executed.

(1) If the car behind the last car of the megajam has a gap $g < v_{\text{max}}$ ahead, it is added to the jam \rightarrow the jam length is increased by 1. This is repeated down to the first car with a gap $g \geq v_{\text{max}}$.

(2) If the first car of the jam reaches $v = v_{\text{max}}$, it leaves the jam; f and l are both decreased by 1.

(3) If the jam has decayed to length 0, the measurement is finished, and τ_J is set to the current time; else, return to step 1.

If the megajam did not dissolve after a certain cutoff time t_{cut} , the algorithm was stopped, and τ_J was set to t_{cut} . For each value of ρ , the measurement was averaged over M runs. In the case of the data presented in Fig. 7, the values were $t_{\text{cut}} = 30L$ and $M = 100$.

[1] *Traffic and Granular Flow*, edited by D.E. Wolf, M. Schreckenberg, and A. Bachem (World Scientific, Singapore, 1996).
 [2] *Traffic and Granular Flow '97*, edited by M. Schreckenberg and D.E. Wolf (Springer, Singapore, 1998).
 [3] D. Helbing, *Verkehrsdynamik: Neue physikalische Modellierungskonzepte* (Springer, Berlin, 1997).
 [4] J. Krug, Phys. Rev. Lett. **67**, 1882 (1991); M.R. Evans, D.P. Foster, C. Godrèche, and D. Mukamel, *ibid.* **74**, 208 (1995);

M.R. Evans, Y. Kafri, H.M. Koduvely, and D. Mukamel, *ibid.* **80**, 425 (1998).
 [5] K. Nagel and M. Schreckenberg, J. Phys. I **2**, 2221 (1992).
 [6] K. Nagel, Phys. Rev. E **53**, 4655 (1996).
 [7] K. Nagel and H.J. Herrmann, Physica A **199**, 254 (1993).
 [8] K. Nagel, Int. J. Mod. Phys. C **5**, 567 (1994).
 [9] S. Wolfram, Rev. Mod. Phys. **55**, 601 (1983).
 [10] J. Krug and H. Spohn, Phys. Rev. A **38**, 4271 (1988).

- [11] O. Biham, A.A. Middleton, and D. Levine, *Phys. Rev. A* **46**, R6124 (1992).
- [12] V. Belitsky and P.A. Ferrari, *J. Stat. Phys.* **80**, 517 (1995).
- [13] Y. Elskens and H.L. Frisch, *Phys. Rev. A* **31**, 3812 (1985).
- [14] Already the presence of three velocities leads to completely different behavior, see P. Krapivsky, S. Redner, and F. Leyvraz, *Phys. Rev. E* **51**, 3977 (1995).
- [15] L.C.Q. Vilar and A.M.C. de Souza, *Physica A* **211**, 84 (1994).
- [16] B. Eisenblätter, L. Santen, A. Schadschneider, and M. Schreckenberg, *Phys. Rev. E* **57**, 1309 (1998).
- [17] G. Csányi and J. Kertész, *J. Phys. A* **28**, L427 (1995); **29**, 471(E) (1996).
- [18] M. Sasvári and J. Kertész, *Phys. Rev. E* **56**, 4104 (1997).
- [19] D. Chowdhury, K. Ghosh, A. Majumdar, S. Sinha, and R.B. Stinchcombe, *Physica A* **246**, 471 (1997).
- [20] S. Lübeck, M. Schreckenberg, and K.D. Usadel, *Phys. Rev. E* **57**, 1171 (1998); and in [2], p. 361.
- [21] L. Roters, Diploma thesis, University of Duisburg, 1998 (unpublished).
- [22] S. Lübeck, L. Roters, and K.D. Usadel, in [2], p. 355.
- [23] H. Yaguchi, *Hiroshima Math. J.* **16**, 449 (1986).
- [24] A. Schadschneider and M. Schreckenberg, *J. Phys. A* **26**, L679 (1993).
- [25] M. Schreckenberg, A. Schadschneider, K. Nagel, and N. Ito, *Phys. Rev. E* **51**, 2939 (1995).
- [26] J. Krug and P.A. Ferrari, *J. Phys. A* **29**, L465 (1996).
- [27] M.J. Lighthill and G.B. Whitham, *Proc. R. Soc. London, Ser. A* **229**, 317 (1955).
- [28] H. van Beijeren, R. Kutner, and H. Spohn, *Phys. Rev. Lett.* **54**, 2026 (1985).
- [29] D. Forster, D.R. Nelson, and M.J. Stephen, *Phys. Rev. A* **16**, 732 (1977).
- [30] M. Kardar, G. Parisi, and Y.C. Zhang, *Phys. Rev. Lett.* **56**, 889 (1986).
- [31] T. Nagatani, *J. Phys. A* **28**, 7079 (1995).
- [32] J. Krug and H. Spohn, *Europhys. Lett.* **8**, 219 (1989).
- [33] K. Nagel and M. Paczuski, *Phys. Rev. E* **51**, 2909 (1995).
- [34] B. Eisenblätter, Diploma thesis, University of Duisburg, 1996 (unpublished).
- [35] In many cases ρ'_c was observed to be close to the critical density ρ_c^0 of the deterministic model.